Ultra-Broadband and Electro-Optical Tunable Absorption in Double-Walled Carbon Nanotubes

Diao Li, Mohsen Ahmadi, Qiang Zhang, Peng Liu, Zhenyu Xu, Nan Wei, Esko I. Kauppinen, and Zhipei Sun

(Invited Paper)

***Abstract*—Electro-optical modulators are critical elements in the rapidly developing data communication, optical interconnects, silicon-based photonic systems and terahertz technologies. The limited optoelectronic properties and complicated material growth in traditional semiconductors hinder the rapidly surging demand for modulator performance, energy efficiency, cost, etc. The emergence of two-dimensional materials and one-dimensional carbon nanotubes in recent decades has brought new opportunities with their tremendous selection degree of freedom for exceptional optoelectronic properties. In this article, we present ultra-broadband and electro-optical tunable absorption modulators by employing double-walled carbon nanotube films in a capacitor geometry, spanning the visible to terahertz spectra. The formation of supercapacitors around the ionic gel electrolyte and carbon nanotube film interfaces accounts for the large carrier transition and optical conductivity change, which behaves a thickness dependent electroabsorption dynamics. Our findings not only broaden the understanding of low-dimensional material applications in electro-optics but also pave the way for future developments in high-performance broadband modulators.**

***Index Terms*—One-dimensional materials, double-walled carbon nanotube, electro-optical modulator.**

Manuscript received 13 February 2024; revised 9 July 2024; accepted 12 July 2024. Date of publication 16 July 2024; date of current version 1 August 2024. This work was supported in part by the Academy of Finland under Grant 314810, Grant 333982, Grant 336144, Grant 352780, Grant 352930, and Grant 353364, in part by the Academy of Finland Flagship Programme under Grant 320167, PREIN, in part by the EU H2020-MSCA-RISE-872049 (IPN-Bio), in part by the Jane and Aatos Erkko foundation and the Technology Industries of Finland centennial foundation (Future Makers 2022), and in part by ERC under Grant 834742. *(Corresponding authors: Diao Li; Qiang Zhang; Esko I. Kauppinen; Zhipei Sun.)*

Diao Li and Mohsen Ahmadi are with the Department of Electronics and Nanoengineering, Aalto University, FI-00076 Espoo, Finland (e-mail: lidiaoxc@163.com; ahmadi.mohsen1714@gmail.com).

Qiang Zhang, Zhenyu Xu, Nan Wei, and Esko I. Kauppinen are with the Department of Applied Physics, Aalto University, FI-00076 Espoo, Finland (e-mail: qiang.zhang@aalto.fi; zhenyu.xu@aalto.fi; weynan@pku.edu.cn; esko.kauppinen@aalto.fi).

Peng Liu is with the Department of Electronics and Nanoengineering, Aalto University, FI-00076 Espoo, Finland, and also with the Department of Applied Physics, Aalto University, FI-00076 Espoo, Finland (e-mail: peng.1.liu@aalto.fi).

Zhipei Sun is with the Department of Electronics and Nanoengineering, Aalto University, FI-00076 Espoo, Finland, and also with the QTF Centre of Excellence, Department of Applied Physics, Aalto University, FI-00076 Espoo, Finland (e-mail: zhipei.sun@aalto.fi).

Color versions of one or more figures in this article are available at https://doi.org/10.1109/JSTQE.2024.3429414.

Digital Object Identifier 10.1109/JSTQE.2024.3429414

I. Introduction

OPTICAL modulators, a critical component to manipulate the physical parameters of light, are indispensable in photonic and optoelectronic systems. The most developed optical modulators adopt electro-optical approach to convert electrical signal to optical signal, which thus can be used in telecommunication, optical computing, optical signal processing [1], [2], [3], etc. These technologies are based on traditional semiconductors owning advanced optoelectronic behaviors. Representatives are III-V group compounds (e.g., GaAs, InP), lithium niobate, and silicon-based photonic platforms [4], [5], [6]. The increasing demand for high-efficiency, fast speed, low energy consumption and miniaturized modulators has directed huge research efforts in silicon-based photonic platforms because of their merits for wafer-scale integration and compatibility to the mature complementary metal-oxide semiconductor technology [7]. According to the parameters being affected by the electrical potential, one can modulate intensity (amplitude), phase or polarization of the light passing through the active material in the device [8]. Intensity modulation, a fundamental regime usually accomplished by changing the light absorption of a component in photonic system, has been an essential need for many applications. The realization of absorption modulation relies on modifying the charge carrier density of the sensitive material, which is often utilized as electrodes in the modulator. Although were drastically developed, the electro-optical absorption modulation with traditional bulk semiconductors are still restricted in operation bandwidth, and need large driving voltage, which is attributed to the large bandgap and low doping efficiency. The emergence of a number of two-dimensional (2D) nanomaterials, graphene [9], [10], [11] and its analogue (e.g., transition metal dichalcogenides of MoS_2, WS_2, $MoSe_2$, WSe_2) [12], [13], [14], [15] finds alternative option for improved performance. The combination of gapless graphene and gap tunable transition metal dichalcogenides greatly extends the absorption range, but the insufficiency of density of states around the Fermi level confines their gate dependent doping concentration, and gives weak absorption effect along ultrathin atomic layer. Effective strategies (e.g., waveguide integration, heterostructures, plasmon oscillator) [16], [17], [18] have been proposed to enhance the interaction intensity, but in the cost of limited bandwidth and complicated fabrication process.

In quasi one-dimensional carbon nanotube, optoelectronic properties and band structures change dramatically as a result of quantum confinement and curvature, in comparison to 2D nanomaterials. The valence or conduction bands are composed of discrete levels called subbands, and have different azimuthal quantum members. Carrier transition of external excitation can be interband or intersubband. In addition, the absorption spectrum variation under electrical field is significantly enhanced by excitonic effects [19]. Compared to bulk semiconductors and graphene, the typical absorption spectrum of single walled carbon nanotubes (SWCNTs) behaves multiple characteristic peaks corresponding to the transition between van Hove singularities in the density of states [20]. Benefit from the development in material synthesis, SWCNTs have been widely studied as an active medium to acquire optical modulation from the near infrared to mid-infrared region [21], [22]. Investigations also reveal the existence of plasmon conductivity peaks in metallic and doped semiconducting carbon nanotubes at the THz frequency range [23], indicating that carbon nanotube is a promising building block for THz devices. In comparison with the massive research attention attracted by SWCNTs, the investigation about structure and properties of double walled carbon nanotubes (DWCNTs) is a relatively less touched area until the synthesis and separation of its high purity sample [24], [25]. In a simplified model, the optical absorption spectrum of DWCNTs can be described as a superposition of the spectra of its inner and outer tubes, and a small shift of absorption peaks caused by van der Waals interaction between the two adjacent walls [26], [27], [28], [29]. Experimental observation in our previous work shows that the absorption peaks contributed by SWCNTs are significantly suppressed if the catalyst concentration during the synthesis can be controlled appropriately [30]. Notably that the outer walls of DWCNTs are quite large in diameter and have wide distribution, while the inner walls are in a comparable size of small individual SWCNTs. As a result, bandgaps of DWCNTs are much smaller than their single walled counterparts and the optical absorption spectrum of DWCNTs can be drastically broadened.

In this work, we present our recent demonstration of ultra-broadband and electro-optical tunable absorption in DWCNTs. A pair of DWCNT films are utilized as active electrodes, and isolated by a thin layer of ionic gel electrolyte to form a capacitor device. Electrical gating introduced carrier concentration reconfiguration on the nanotube film contributes to the absorption variation from the visible to mid-infrared. Drude-like conductivity change of the DWCNT films is in charge of the THz wave modulation. In particular, our result shows a thickness-dependent electro-optical absorption change over the entire spectrum range, giving alternative solution for modified efficiency in modulation strength.

II. Electro-Optical Absorption Modulator With Carbon Nanotube

A. Material Synthesis and Characterization

The synthesis of DWCNTs was carried out with the floating catalyst chemical vapor deposition (FC-CVD) method. A schematic experimental setup is illustrated in Fig. 1(a). Gas-phase precursors, including ferrocene ($FeCp_2$), sulfur, CH_4 and carrier gases of N_2 and H_2 were introduced to generate DWCNTs in the reactor at 1100 °C. Aerosol-like DWCNTs were covalently constructed in gas-phase, and collected as large area continuous network by dry filtration from the outlet of the reactor with a membrane filter at room temperature, as shown in Fig. 1(b). The deposited film thickness can be flexibly tailored by setting the collection time. During the reaction process, it is possible to control the ratio between SWCNTs and DWCNTs by adjusting the concentration of the catalyst ($FeCp_2$). As the increase of catalyst concentration, the produced nanotubes change from SWCNTs in large bundles to DWCNTs in small bundles. In experiment, the concentration of catalyst was determined by controlling its evaporation temperature. When the temperature is over 35 °C (selected in this work), the Van Hove transition peaks in the absorption spectrum of the nanotubes disappear completely, indicating high-concentration DWCNTs are synthesized. Statistical analysis result in our previous report [30] shows that only ∼5% are SWCNTs, and the others are DWCNTs and their bundles. For the DWCNTs, most of the tube length is from ∼1 μm to ∼40 μm, giving a mean length of ∼20(±11) μm. The identification of DWCNTs was carried out by Raman spectroscopy (Horiba LabRAM HR 800) under the excitation of a 633-nm continuous-wave laser. Fig. 1(c) shows the Raman spectrum with radial breathing mode (RBM) at ∼221.8 cm^{-1}, disordered carbons caused vibration mode (D band) at ∼1325 cm^{-1} and tangential oscillation mode (G band) at ∼1588 cm^{-1}. The single Raman peak of the G band with a Lorentzian line-shape indicates that the excitation is from semiconducting nanotubes [31]. A further nanoscale investigation was conducted by scanning electron microscope (SEM, ZEISS Sigma VP, 1.0 kV) and high-resolution transmission electron microscope (HR-TEM, JEOL JEM-2200FS, 200 kV). Experimental results are shown in Fig. 1(d) and (e), respectively. The SEM morphology manifests homogenous nanotube networks, which is a result of random

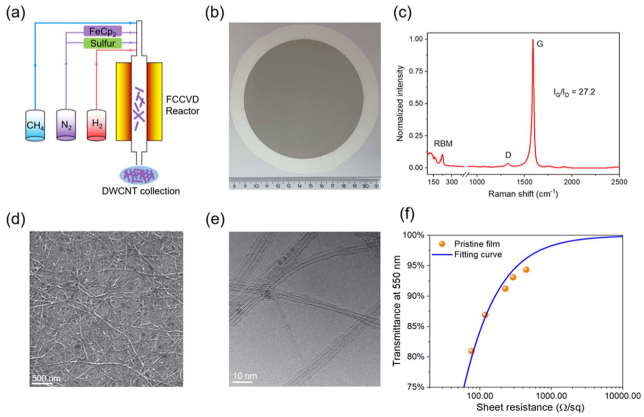

Fig. 1. (a) Schematic setup of the FC-CVD method for DWCNT synthesis and film deposition. (b) A large-scale DWCNT thin film collected on a membrane filter. (c) Raman spectroscopy of the synthesized DWCNTs film (excited by a 633 nm laser). (d) SEM and (e) HR-TEM images of the DWCNT film. (f) Transmittance of DWCNT films at 550 nm as a function of their sheet resistance.

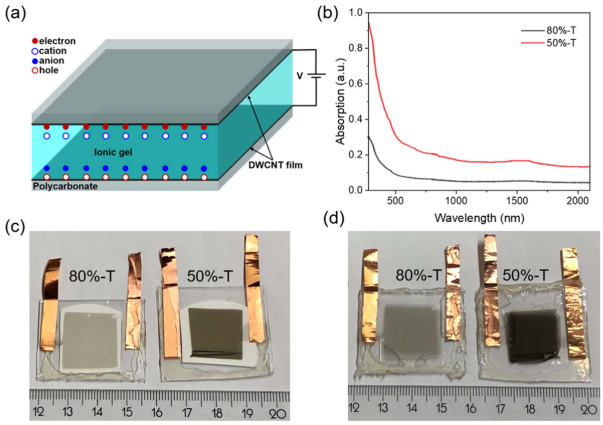

Fig. 2. (a) Schematic of the capacitive modulator. A pair of DWCNT films are employed as parallel board electrodes and spaced by ionic gel electrolyte. Supercapacitive fields were formed by electron-cation and anion-hole concentration around the DWCNT films when gate is applied. (b) Optical absorption spectra of the pristine DWCNT films in different thicknesses corresponding to ~80% (black curve) and 50% (red curve) transmittances at 550 nm wavelength. (c), (d). Pictures of the prepared devices without ionic gel electrolyte (c) and with ionic gel electrolyte (d).

orientation during the collection process. In Fig. 1(e), the HR-TEM image verifies the formation of two embedded nanotubes. The black particles on the nanotubes are from the residual catalyst of ferrocene. We measured the pristine film transmittance at 550 nm laser and corresponding sheet resistance with different samples; experimental data are plotted in Fig. 1(f). The fitted curve shows that the film transmittance increases exponentially against the sheet resistance. This is attributed to the increased carrier concentration when the film becomes thicker (and vice versa). Note that the sheet resistance can be less than 100 Ω/sq when the transmittance is approximately below 83%, which proves the high quality of the DWCNT films.

B. Modulator Fabrication

The modulator device was configured in a capacitor geometry by placing two DWCNT thin films in parallel and isolated by ionic gel electrolyte (1-Ethyl-3-methylimidazolium bis(trifluoromethyl sulfonyl)imide, i.e., EMIM-TFSI). A schematic diagram of the device is shown in Fig. 2(a). Two DWCNT films (2×2 cm^2) were transferred to transparent polycarbonate boards. A pair of copper foil stripes were connected to the edge of each DWCNT thin film on the substrates for voltage application. Two polycarbonate substrates with the DWCNT film side were put together to form a 125 μm spacer. A completed device was acquired after injecting the ionic gel solution. For comparison, two devices utilizing 80% and 50% transmittance DWCNT films at 550 nm wavelength were prepared. The film thicknesses were evaluated as ~29 nm for the 80% transmittance and ~80 nm for the 50% transmittance with atomic force microscopy. Fig. 2(b) shows the optical absorption spectra of the selected DWCNT films (carried by Perkin-Elmer Lambda 950, UV-VIS-NIR spectrometer) in the wavelength range from 280 nm to 2100 nm. The absorption spectra exhibit smooth intensity distribution, which is a comprehensive result of two factors. One is the wide outer tube diameter distribution ranging from ~2 nm to ~6 nm in our DWCNT films, as shown in the Supporting Information of our previous work [30]. The large outer walls of the DWCNTs form very small bandgaps. The other one comes from the excitonic transition energies of both the inner and outer walls when the outer tube is semiconducting type (i.e., the inner tube can be semiconducting or metallic). The combination of different charge transfer behaviors between the tubes also contributes to the broadband optical absorption of the DWCNTs. Fig. 2(c) presents the two modulators utilizing DWCNT films with 80% (left) and 50% (right) transmittance at 550 nm wavelength before the injection of ionic gel electrolyte. The grey and dark grey areas are the DWCNT electrodes with different transparencies. The white membrane under the nanotube film is an isolation layer to prevent short-circuit, which turns transparent after injecting the ionic gel, as shown in Fig. 2(d).

C. Electro-Optical Modulation From the Visible to Infrared Light

In silicon-based modulators, electrical field is generated between electrodes spaced by dielectric, this limits the formation of large concentration carrier doping in the active material because of the dielectric breakdown issue [32]. It is therefore challenging to realize modulation at high frequency range around near infrared and visible light. In comparison, ionic gel electrolyte with large electrochemical window has been demonstrated viable, alternative to extend the electroabsorption modulation range [33]. Cations and anions in the electrolyte offer a regime to form supercapacitor at the DWCNT film surfaces, which is confined to nanometer thickness. Together with the huge surface to volume ratio of DWCNT film, the strong localized field built by the supercapacitor enables storing drastically large density carrier at the film interfaces. This mechanism ensures the electro-optical modulation broadening to visible wavelengths under gate of only several volts. On the other hand, the interband absorption in the mid-infrared range can be Pauli blocked by natural doping to the nanotube films. This influence was suppressed by baking the device at 150 °C for 30 minutes before injecting the ionic gel, and the remaining fabrication was completed in a glove box filled with nitrogen gas to prevent ionic gel oxidation and device degradation. Fig. 3 presents the change of transmission as a function of gate voltage between −2.1 and 2.1 V. The transmission spectra were normalized with the spectrum measured at open circuit voltage. All these transmission spectra have subtracted the interference from the substrate materials (i.e., a reference device without DWCNT electrodes), ensuring that the gate dependent transmission variation is solely contributed by the DWCNT films. Fig. 3(a) shows a symmetric mapping of transmission change against voltage from the thinner sample (i.e., DWCNT film of 80% transmittance at 550 nm), but with the symmetry center slightly shifted to 0.3 V, due to charge impurities in the ionic gel and substrates. The maximum change in the transmission is about 6.6% at 2.1 V gate voltage, which presents a blue-shift as the increase of electrical gating, see Fig. 3(b). This phenomenon is attributed to the large interband transition around the Fermi energy when the gate voltage is increased.

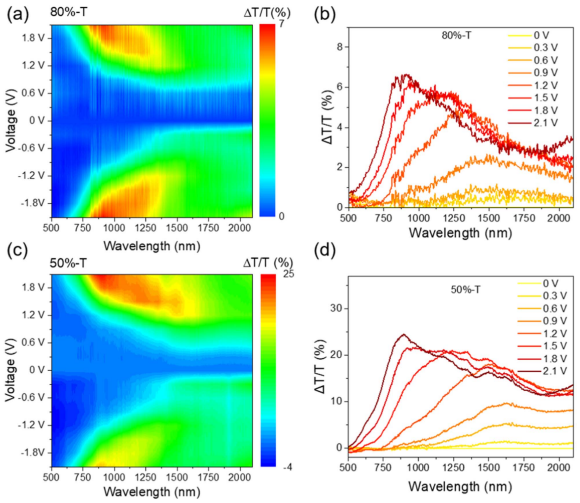

Fig. 3. (a) Normalized transmission change of the device (with 80% transmittance of DWCNT films) plotted as functions of wavelength and gate voltage. (b) The variation of normalized transmission as a function of wavelength and positive voltage (with 80% transmittance of DWCNT films). (c) Normalized transmission change of the device (with 50% transmittance of DWCNT films) plotted as functions of wavelength and gate voltage. (d) The variation of normalized transmission as a function of wavelength and positive voltage (with 50% transmittance of DWCNT films).

Nevertheless, the transmission change in longer wavelengths starts to saturate from 1.2 V, and the transmission comes to a reverse change tendency at 2.1 V, which is probably a behavior caused by the quantum confined Stark effect in the semiconductor nanotubes. A further extension to the gate voltage intensity will induce irreversible degradation of the electrolyte. Thus, the amplitude modulation is also limited. Note that further increase in modulation intensity is not constrained by the nanotube material, whereas the film thickness might be an additional degree of freedom for more efficient modulation at the same gate voltage.

A comparison experiment was carried out in another device by replacing the DWCNT electrodes with thicker films (i.e., DWCNT film of 50% transmittance at 550 nm). The mapping graph and transmission change against gate voltage are illustrated in Fig. 3(c) and (d). The transmission change as a function of the gate turns asymmetric, which can be attributed to a memory effect caused by multiple measurements. In experiment, we first carried out the positive gate voltage dependent transmission spectra for several times to identify its reproductivity. These multiple measurements introduced residual electrical doping to the DWCNT films when the gate is unapplied. The followed transmission spectra measurement in negative gate voltage drops in efficiency because part of the potential was used to remove the residual doping in reverse gate. This memory effect looks more pronounced in thicker DWCNT films compared to the mapping in Fig. 3(a). In contrast to the spectrum distribution in Fig. 3(b), the result in Fig. 3(d) gives an absorption modulation increase to ∼24.4% at maximum, identifying that the modulation is thickness-dependent in our devices. For clarification, the tiny spikes of the spectra in Fig. 3(b) are from the random background noise of the white light source in the UV-VIS-NIR spectrometer rather than the device.

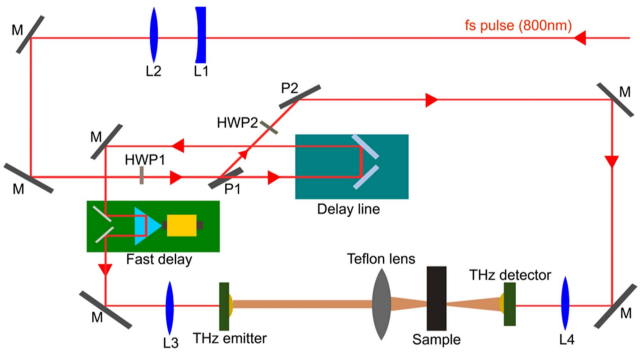

Fig. 4. Schematic representation of the THz time domain spectroscopy and detection system. M, reflection mirror; L1, L2, L3, L4, collimation and focus lenses. HWP1, HWP2, half-wave plates; P1, P2, polarizers.

D. Electro-Optical Modulation at Terahertz Wave

Electro-optical response of the DWCNT modulator was also characterized with a THz time-domain spectroscopy and detection system in the frequency range of ∼0.2–1.05 THz. We measured the time-domain spectrum variation as a function of the gate voltages within −2.1 to 2.1 V. The experimental setup is drawn in Fig. 4. THz wave was acquired from a GaAs photoconductive emitter under the nonlinear excitation of femtosecond pulses (800 nm, 150 fs, 78 MHz) generated in a mode-locked Ti: sapphire laser. The incident laser pulses are guided to a compressing/expanding telescope (L1, L2) to get ∼3 mm beam size in diameter. Half-wave plate HWP1 and polarizer P1 are utilized to split the laser beam for pumping of the THz emitter. The power can be adjusted by tuning the angle of HWP1. The split beam is then guided to an optical delay line and a fast delay line, both are based on hollow retro-reflector. The retro-reflector of the fast delay line is mounted on a fast translation voice coil stage, which enables 10 times moving per second. The beam is then focused by lens L3 to the THz emitter as pump excitation. On the other hand, the half-wave plate HWP2 and polarizer P2 are used to adjust the beam power pumped to the THz detector. Lens L4 focuses the beam to the THz detector (photoconductive antenna). The time-domain spectrum test can be obtained by placing the sample between the THz emitter and detector. In addition, a Teflon lens is used after the THz emitter to get a focused beam at the sample position. The entire setup shown in Fig. 4 was placed in a closed chamber pumped with nitrogen gas to eliminate the influence of ambient humidity.

Time-domain electrical field variation of the transmitted THz signal as a function of gate voltage is shown in Fig. 5(a). Here, the measurement is from the modulator with 80% transmittance DWCNT films. These spectra were then converted to transmission change through the Fourier transform and normalized to the spectrum under the 0 V gate, which are illustrated in Fig. 5(b). It is seen that the maximum change of transmission spectrum does not appear at 0 V. We attribute this to the memory effect introduced from the previous measurements in the visible and infrared range. The peaks with ∼0.5 THz separation in the change of transmission spectrum come from a Fabry-Perot resonance, which is formed by the polycarbonate surfaces.

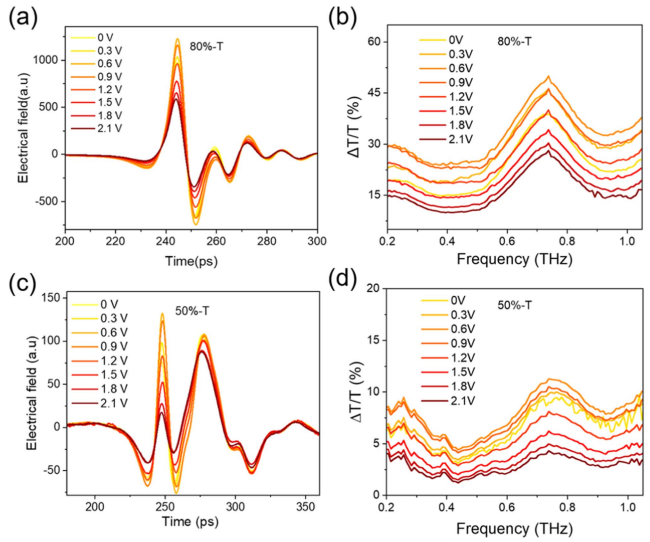

Fig. 5. (a) Time-domain electrical field variation of the THz wave as a function of gate voltage, measured with the 80% transmittance of DWCNT films. (b) Normalized transmission change as a function of THz frequency converted from time-domain spectra (in (a)) by Fourier transform. (c) Time-domain electrical field variation of the THz wave as a function of gate voltage, measured with the 50% transmittance of DWCNT films. (d) Normalized transmission change as a function of THz frequency converted from time-domain spectra (in (c)) by Fourier transform.

Over the entire spectrum range, the maximum difference in the gate-dependent transmission change is approximately 32% at 0.75 THz. In comparison, we also characterized the THz time-domain spectrum variation as a function of gate voltage with the device employing 50% transmittance at 550 nm, the result is shown in Fig. 5(c). Again, it is shown that the largest electrical field appears at 0.6 V, which means the nanotube films return to their minimum conductivity. The Fourier transform spectra in Fig. 5(d) shows similar behavior against the result in Fig. 5(b). But, the maximum difference of the transmission change is only 7% at 0.75 THz. Note that the change of transmission spectrum corresponding to gate voltage in Fig. 5(d) is much smaller than that in Fig. 5(b) corresponding to the same voltage. This observation also demonstrates a thickness-dependent modulation in terms of intensity in our supercapacitive modulators. Compared to the infrared and visible spectral results, due to the different mechanisms of optical absorption (film conductivity) in THz range, we observed higher modulation efficiency in the device with thinner DWCNT films rather than the device with thicker film. This can be attributed to the larger conductivity change in a less conductive (thinner) film against a more conductive (thicker) one. Apart from the intensity modulation, time response also matters the performance of the device. The charging time of the carbon nanotube capacitor, defined as RC time constant, is used to evaluate the response frequency. It has been known that ion diffusion imposing a limit to the response time of carbon nanotube capacitors in the range from microsecond to millisecond range [34]. Combine the experimentally measured RC time constant in an analogue graphene-ion liquid capacitor [33], the response frequency of our device can be estimated in several to a few tens Hz range.

In this section, we demonstrate an electro-optical absorption modulator by employing DWCNT nanofilms as electrodes in a capacitive device geometry. Aerosol-like DWCNTs were synthesized in an FC-CVD stove and deposited as nanofilms with controllable thicknesses. Ionic gel electrolyte with large electrochemical window was utilized as spacer in the capacitor for gate-induced supercapacitor at the nanotube interfaces, which was demonstrated as an effective way for large concentration carrier doping under low gate voltages. Our modulators perform gate-dependent transmission modulation from the visible to infrared wavelengths (500–2100 nm) through interband transition and optical conductivity modulation at THz wave (∼0.2–1.05 THz) by intraband transition. The gate-controlled transmission change in our DWCNT films shows thickness-dependent behavior, which increases as a function of thickness in the visible to infrared range while decreases in THz wave. Our results identify that DWCNT is a promising active electro-optical medium for ultra-broadband light manipulation with the combination of controllable intensity, low gate voltage, cost efficiency and easy fabrication.

III. Summary and Perspectives

In summary, we have demonstrated an ultra-broadband electro-optical absorption modulator by using FC-CVD synthesized DWCNTs as active material. The comparison experiment reveals that the intensity modulation of the DWCNT films is thickness-dependent over all the measured spectrum range. In particular, the ultra-broadband absorption modulation is mainly attributed to the formation of electrical double layers at the ionic gel and DWCNT film interfaces. The exponential potential drop cross ultrathin Helmholtz layers ($<$1nm) allows high-density charge accumulation [35] near the DWCNT films, which dominates the absorption extension toward the visible range. It is notable that the electrical double layer is almost independent to the thickness of the ionic gel layer [36]. Nevertheless, in contrast to the fast carrier mobility in DWCNTs, the slow ion diffusion in ionic gel limits the time response of the device. Alternatively, if the ionic gel is replaced by solid dielectric (e.g., Al_2O_3, SiO_2), the device will function as an electrostatic capacitor. In this model, the charge density scales linearly against the applied voltage and the dielectric constant, and it is inversely proportional against the thickness of the spacer between the DWCNT electrodes [37]. In order to obtain broader absorption modulation, three approaches can be used, i.e., select the dielectric material with higher permittivity, reduce the thickness of the spacer, and increase the gate voltage. However, the improvement is limited because of breakdown issue. Therefore, one can hardly achieve absorption modulation in the visible spectrum or even near infrared range with these modulators. Considering that the optical conductivity of DWCNTs is also determined by the charge density, the modulation efficiency in THz wave will decrease. On the other hand, electro-optical modulators with solid dielectric are competitive in applications where high speed response is critical (e.g., ultrafast signal processing). But complicated device design and nanofabrication process bring huge challenges to overcome the RC time constant

bottleneck for high speed operation. Here, we emphasize the ultra-broadband electro-optical absorption modulation (from visible to THz wave) in semiconducting DWCNTs by using ionic gel as dielectric material. Our findings open new avenues in the field of electro-optical modulators, highlighting potential alternatives of using one-dimensional carbon nanotubes, and broadening the spectrum of materials available for advanced photonic applications.

Acknowledgment

The authors would like to thank the Academy of Finland for funding support for the research at Aalto University.

References

[1] G. Reed et al., "Optical modulators," in *Integrated Photonics for Data Communication Applications*. Amsterdam, The Netherlands: Elsevier, 2023, pp. 69–121.
[2] N. L. Kazanskiy, M. A. Butt, and S. N. Khonina, "Optical computing: Status and perspectives," *Nanomaterials*, vol. 12, no. 13, Jun. 2022, Art. no. 2171, doi: 10.3390/nano12132171.
[3] J. Wang and Y. Long, "On-chip silicon photonic signaling and processing: A review," *Sci. Bull.*, vol. 63, no. 19, pp. 1267–1310, Oct. 2018, doi: 10.1016/j.scib.2018.05.038.
[4] B. Bennett and R. Soref, "Electrorefraction and electroabsorption in InP, GaAs, GaSb, InAs, and InSb," *IEEE J. Quantum Electron.*, vol. 23, no. 12, pp. 2159–2166, Dec. 1987, doi: 10.1109/JQE.1987.1073276.
[5] C. Wang et al., "Integrated lithium niobate electro-optic modulators operating at CMOS-compatible voltages," *Nature*, vol. 562, no. 7725, pp. 101–104, Oct. 2018, doi: 10.1038/s41586-018-0551-y.
[6] R. Soref, "The past, present, and future of silicon photonics," *IEEE J. Sel. Topics Quantum Electron.*, vol. 12, no. 6, pp. 1678–1687, Nov./Dec. 2006, doi: 10.1109/JSTQE.2006.883151.
[7] D. Thomson et al., "Roadmap on silicon photonics," *J. Opt.*, vol. 18, no. 7, Jun. 2016, Art. no. 073003, doi: 10.1088/2040-8978/18/7/073003.
[8] Z. Sun, A. Martinez, and F. Wang, "Optical modulators with 2D layered materials," *Nature Photon.*, vol. 10, no. 4, pp. 227–238, Apr. 2016, doi: 10.1038/nphoton.2016.15.
[9] K. S. Novoselov et al., "Electric field effect in atomically thin carbon films," *Science*, vol. 306, no. 5696, pp. 666–669, Oct. 2004, doi: 10.1126/science.1102896.
[10] Q. Bao et al., "Atomic-layer graphene as a saturable absorber for ultrafast pulsed lasers," *Adv. Funct. Mater.*, vol. 19, no. 19, pp. 3077–3083, Oct. 2009, doi: 10.1002/adfm.200901007.
[11] Z. Sun et al., "Graphene mode-locked ultrafast laser," *ACS Nano*, vol. 4, no. 2, pp. 803–810, Jan. 2010, doi: 10.1021/nn901703e.
[12] A. K. Newaz et al., "Electrical control of optical properties of monolayer MoS_2," *Solid State Commun.*, vol. 1, no. 155, pp. 49–52, Feb. 2013, doi: 10.1016/j.ssc.2012.11.010.
[13] C. Cong, J. Shang, Y. Wang, and T. Yu, "Optical properties of 2D semiconductor WS_2," *Adv. Opt. Mater.*, vol. 6, no. 1, Jan. 2018, Art. no. 1700767, doi: 10.1002/adom.201700767.
[14] Z. Luo et al., "Nonlinear optical absorption of few-layer molybdenum diselenide ($MoSe_2$) for passively mode-locked soliton fiber laser," *Photon. Res.*, vol. 3, no. 3, pp. A79–A86, Jun. 2015, doi: 10.1364/PRJ.3.000A79.
[15] J. S. Ross et al., "Electrically tunable excitonic light-emitting diodes based on monolayer WSe_2 p-n junctions," *Nature Nanotech.*, vol. 9, no. 4, pp. 268–272, Apr. 2014, doi: 10.1038/nnano.2014.26.
[16] M. Liu et al., "A graphene-based broadband optical modulator," *Nature*, vol. 474, no. 7349, pp. 64–67, Jun. 2011, doi: 10.1038/nature10067.
[17] S. Rathi et al., "Tunable electrical and optical characteristics in monolayer graphene and few-layer MoS_2 heterostructure devices," *Nano Lett.*, vol. 15, no. 8, pp. 5017–5024, Aug. 2015, doi: 10.1021/acs.nanolett.5b01030.
[18] M. Klein et al., "2D semiconductor nonlinear plasmonic modulators," *Nature Commun.*, vol. 10, Jul. 2019, Art. no. 3264, doi: 10.1038/s41467-019-11186-w.
[19] V. Perebeinos and P. Avouris, "Exciton ionization, Franz-Keldysh, and Stark effects in carbon nanotubes," *Nano Lett.*, vol. 7, no. 3, pp. 609–613, Mar. 2007, doi: 10.1021/nl0625022.
[20] M. G. Burdanova et al., "A review of the terahertz conductivity and photoconductivity of carbon nanotubes and heteronanotubes," *Adv. Opt. Mater.*, vol. 9, no. 24, Dec. 2021, Art. no. 2101042, doi: 10.1002/adom.202101042.
[21] M. L. Moser et al., "Fast electrochromic device based on single-walled carbon nanotube thin films," *Nano Lett.*, vol. 16, no. 9, pp. 5386–5393, Sep. 2016, doi: 10.1021/acs.nanolett.6b01564.
[22] Y. Sun et al., "Large-scale multifunctional carbon nanotube thin film as effective mid-infrared radiation modulator with long-term stability," *Adv. Opt. Mater.*, vol. 9, no. 3, Feb. 2021, Art. no. 2001216, doi: 10.1002/adom.202001216.
[23] Q. Zhang et al., "Plasmonic nature of the terahertz conductivity peak in single-wall carbon nanotubes," *Nano Lett.*, vol. 13, no. 12, pp. 5991–5996, Dec. 2013, doi: 10.1021/nl403175g.
[24] M. H. Endo et al., "'Buckypaper' from coaxial nanotubes," *Nature*, vol. 433, no. 7025, Feb. 2005, Art. no. 476, doi: 10.1038/433476a.
[25] A. A. Green and M. C. Hersam, "Processing and properties of highly enriched double-wall carbon nanotubes," *Nature Nanotechnol.*, vol. 4, no. 1, pp. 64–70, Jan. 2009, doi: 10.1038/nnano.2008.364.
[26] S. Zhao et al., "Rayleigh scattering studies on inter-layer interactions in structure-defined individual double-wall carbon nanotubes," *Nano Res.*, vol. 7, pp. 1548–1555, Aug. 2014, doi: 10.1007/s12274-014-0515-y.
[27] D. I. Levshov et al., "Photoluminescence from an individual double-walled carbon nanotube," *Phys. Rev. B*, vol. 96, no. 19, Nov. 2017, Art. no. 195410, doi: 10.1103/PhysRevB.96.195410.
[28] H. N. Tran et al., "Quantum interference effects on the intensity of the G modes in double-walled carbon nanotubes," *Phys. Rev. B*, vol. 95, no. 20, May 2017, Art. no. 205411, doi: 10.1103/PhysRevB.95.205411.
[29] K. H. Liu et al., "Van der Waals-coupled electronic states in incommensurate double-walled carbon nanotubes," *Nature Phys.*, vol. 10, no. 10, pp. 737–742, Oct. 2014, doi: 10.1038/nphys3042.
[30] Q. Zhang et al., "Large-diameter carbon nanotube transparent conductor overcoming performance-yield tradeoff," *Adv. Funct. Mater.*, vol. 32, no. 11, Mar. 2022, Art. no. 2103397, doi: 10.1002/adfm.202103397.
[31] S. M. Bose, S. Gayen, and S. N. Behera, "Theory of the tangential G-band feature in the Raman spectra of metallic carbon nanotubes," *Phys. Rev. B*, vol. 72, no. 15, Oct. 2005, Art. no. 153402, doi: 10.1103/PhysRevB.72.153402.
[32] F. Palumbo et al., "A review on dielectric breakdown in thin dielectrics: Silicon dioxide, high-k, and layered dielectrics," *Adv. Funct. Mater.*, vol. 30, no. 18, May 2020, Art. no. 1900657, doi: 10.1002/adfm.201900657.
[33] E. O. Polat and C. Kocabas, "Broadband optical modulators based on graphene supercapacitors," *Nano Lett.*, vol. 13, no. 12, pp. 5851–5857, Dec. 2013, doi: 10.1021/nl402616t.
[34] B. Arkook and M. Chen, "Dynamic performance of hybrid infrared modulator based on single-walled carbon nanotubes and ionic liquid enabling fast response," *Adv. Photon. Res.*, vol. 5, no. 2, Feb. 2024, Art. no. 2300210, doi: 10.1002/adpr.202300210.
[35] M. V. Fedorov and A. A. Kornyshev, "Ionic liquid near a charged wall: Structure and capacitance of electrical double layer," *J. Phys. Chem. B*, vol. 112, no. 38, pp. 11868–11872, Sep. 2008, doi: 10.1021/jp803440q.
[36] T. Fujimoto and K. Awaga., "Electric-double-layer field-effect transistors with ionic liquids," *Phys. Chem. Chem. Phys.*, vol. 15, no. 23, pp. 8983–9006, Apr. 2013, doi: 10.1039/C3CP50755F.
[37] C. C. Lee, S. Suzuki, W. Xie, and T. R. Schibli, "Broadband graphene electro-optic modulators with sub-wavelength thickness," *Opt. Exp.*, vol. 20, no. 5, pp. 5264–5269, Feb. 2012, doi: 10.1364/OE.20.005264.

Diao Li received the B.S. degree in physics and the Ph.D. degree in optics from Northwest University, Xi'an, China, in 2011 and 2018, respectively. From 2014 to 2016, he was a visiting Ph.D. student with Aalto University, Espoo, Finland. In 2018, he started his career as a Postdoctoral Researcher with the University of Cambridge, Cambridge, U.K., where he led the ultrafast light sources research project under the European Union Graphene Flagship in Cambridge Graphene Centre. From 2020 to 2023, he was a Staff Scientist with the Department of Electronics and Nanoengineering, Aalto University, where he was a coordinator of the Flagship for Photonics Research and Innovation (PREIN) funded by the Academy of Finland. He is the author of more than 40 research papers, one book chapter and five patents. His research interests include ultrafast lasers, optical modulators and nonlinear optics based on low dimensional nanomaterials, such as carbon nanotube, graphene, and black phosphorus.

Mohsen Ahmadi received the graduation degree (with Hons.) degree in solid state physics from the University of Kurdistan, Erbil, Iraq, in 2019, and the Ph.D. degree from Aalto University, Espoo, Finland, from 2020 to 2022. He is currently a devoted Physicist specializing in terahertz technology. Throughout his doctoral research, he delved into terahertz technology, mainly focusing on areas, such as time-domain spectroscopy, terahertz detectors, and material characterization in the terahertz domain. His work underscores a modest commitment to advancing our understanding of these technologies, employing a meticulous approach, and maintaining a continuous willingness to learn.

Qiang Zhang received the B.S. degree in physics from the Ocean University of China, Qingdao, China, in 2010, and the Ph.D. degree in condensed matter physics from the Institute of Physics, Chinese Academy of Sciences, Beijing, China, in 2016. From 2016 to 2021, he was a Postdoctoral Researcher with Aalto University, Helsinki, Finland. Since 2021, he has been a Senior Scientist/Project Leader with Honda Research Institute, San Jose, CA, USA. He is the author of more than 60 articles, and 15 patents. His research interests include low-dimensional nanomaterials synthesis, multifunctional fibers and electrodes, and applications in sensors and energy devices.

Peng Liu received the B.S. degree in functional materials from Huaqiao University, Xiamen, China, in 2017, and the M.S. degree in chemical engineering from Xiamen University, Xiamen, in 2020. He is currently working toward the Ph.D. degree in engineering physics with Aalto University, Espoo, Finland. His research focuses on the controlled synthesis, applications, and mechanistic studies of carbon nanotubes utilizing the floating catalyst chemical deposition method. Particularly, he specializes in the controllable synthesis and chiral characterization of single-walled carbon nanotubes possessing semiconductor properties. His work extends to the practical application of these nanotubes in flexible electronic devices, including transistors, optoelectronics, and gas sensors.

Zhenyu Xu received the B.E. degree in materials science and Engineering from the China University of Geosciences, Wuhan, China, in 2017, and the M.S. degree in optics from Shenzhen University, Shenzhen, China, in 2020. He is currently working toward the Ph.D. degree in applied physics with Aalto University, Espoo, Finland. His research interests include the synthesis and growth of carbon nanotubes (CNTs) in floating catalyst chemical vapor deposition, chirality identification of double-walled and single-walled CNTs, and patterning techniques and applications of CNT electrodes.

Nan Wei received the B.Eng. degree in electronic engineering from Tsinghua University, Beijing, China, in 2011, and the Ph.D. degree in physical electronics from Peking University, Beijing, in 2016.

From 2016 to 2020, he was a Postdoctoral Researcher with the Department of Applied Physics, Aalto University, Espoo, Finland. Since 2020, he has been an Assistant Research Professor with the Research Center for Carbon-based Electronics, Peking University.

He is the author of more than 50 research papers and more than ten patents. His research interests include carbon-based devices and circuits, reliable systematic measurement, and the development of characterization and demonstration systems.

Dr. Wei was the recipient of the Best Young Scientist Oral Presentation Award (NPO2018, Finland), and Guanghua Scholarship Award (Peking University).

Esko I. Kauppinen received the Ph.D. degree in physics from the University of Helsinki, Helsinki, Finland, in 1992. He is currently the Head of the Nano Materials Group and the Tenured Professor with the Department of Applied Physics, School of Science, Aalto University, Espoo, Finland. He has authored or coauthored more than 500 scientific journal papers such as, in science, nature nanotechnology, advanced materials, nano letters, ACS nano, angewandte chemie, carbon, energy, and environmental sciences, having Hirsch-index (Google) more than 87 and more than 29 000 citations. He has given more than 130 keynote and invited conference talks and more than 230 talks at companies. He is considered one of the world leading authors in the areas of single walled carbon nanotube synthesis, characterization and thin film applications. He is the founding member of the companies Canatu Oy (http://www.canatu.com) and MetalCirc Oy (https://www.metalcirc.com/). He is the first Finnish recipient of a UNESCO Nanosciences Medal, which he received in 2018. He is the member of the Finnish Academy of Science and Letters.

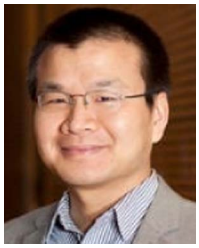

Zhipei Sun received the Ph.D. degree from the Institute of Physics, Chinese Academy of Sciences, Beijing, China, in 2005. He began his career as a Research Fellow with the ICFO - The Institute of Photonic Sciences, Barcelona, Spain, and the University of Cambridge, Cambridge, U.K., where he worked on advanced materials for photonic applications. He is currently a Professor of photonics and the Head of the Photonics Research Group, Department of Electronics and Nanoengineering, Aalto University, Espoo, Finland. He is actively involved with the European Research Council advanced grant, European quantum flagship, Academy of Finland Photonics Flagship, and Academy of Finland Centre of Excellence on quantum technology. His research interests include nonlinear optics, nanophotonics, and ultrafast photonics.